Preparation and Characterization of $\{[M(dmb)_2]TCNQ\cdot xTCNQ^\circ\}_n$ Polymers (M = Cu,Ag; dmb = 1,8-Diisocyano-*p*-menthane; $x = 0, 0.5, 1.0, 1.5$; TCNQ = 7,7,8,8-Tetracyano-*p*-quinodimethane) and Design of New Semi- and Photoconducting Organometallic Materials†

Daniel Fortin, Marc Drouin,‡ and Pierre D. Harvey*

Département de Chimie, Université de Sherbrooke, Sherbrooke (Québec), J1K 2R1 Canada

Received August 12, 1999

New thermoplastic organometallic materials of the type $\{[M(dmb)_2]TCNQ\cdot xTCNQ^\circ\cdot y$ solvent$\}_n$ (M = Cu(I), Ag(I); dmb = 1,8-diisocyano-*p*-menthane; TCNQ = 7,7,8,8-tetracyano-*p*-quinodimethane, $x = 0, 0.5, 1.0, 1.5$; solvent = none, THF or toluene) have been prepared and characterized from X-ray powder diffraction patterns, X-ray crystallography (for some Ag polymers), DSC, and conductivity measurements. While the $\{[M(dmb)_2]TCNQ\cdot xTCNQ^\circ\}_n$ polymers (M = Cu,Ag; $x = 0, 0.5$) are insulating, the others ($x = 1.0$ and 1.5) are semiconducting, and the relative conductivity is found to be a function of the molecular weight and crystallinity. The $\{[Cu(dmb)_2]TCNQ\cdot 1.5TCNQ\}_n$ material is also photoconducting, while the Ag analogue is not. Photochemical and luminescence quenching experiments in the solid-state established that the Cu^+ center and TCNQ° act as electron donor and acceptor, respectively, in this photoprocess. Finally photocells of the type glass/SnO_2/$\{Cu(dmb)_2]TCNQ\cdot TCNQ^\circ\}_n$ + 0.5 acceptor/Al (acceptor = TCNQ°, C_{60} and TCNN (13,13,14,14-tetracyano-5,12-naphthacenequinodimethane)) have been designed and characterized. The quantum yields (number of photoproduced electrons/number of photons) are as follows: TCNQ, 1.6×10^{-4}, C_{60}, 5×10^{-5}, TCNN, 3.0×10^{-4} at λ_{exc} = 330 nm. X-ray data for $\{[Ag(dmb)_2]TCNQ\cdot 2THF\}_n$: space group $P2_1/c$, monoclinic, $a = 13.5501(10)$, $b = 9.9045(10)$, $c = 32.564(2)$ Å, $\beta = 91.130(10)^o$, $Z = 4$. X-ray data for $\{[Ag(dmb)_2]TCNQ\cdot 0.5TCNQ^\circ\cdot 0.5$ toluene$\}_n$: space group $P2_1/c$, monoclinic, $a = 14.3669(19)$, $b = 9.1659(3)$, $c = 34.012(3)$ Å, $\beta = 92.140(8)^o$, $Z = 4$. X-ray data for $\{[Ag(dmb)_2]TCNQ\cdot 1.5TCNQ^\circ\}_n$: space group $C2/c$, monoclinic, $a = 25.830(11)$, $b = 9.680(2)$, $c = 42.183(19)$ Å, $\beta = 104.87(4)^o$, $Z = 8$. X-ray data for $\{[Ag(dmb)_2]DCTC\}_n$: space group $P2_1/a$, monoclinic, $a = 26.273(3)$, $b = 9.730(3)$, $c = 31.526(3)$ Å, $\beta = 112.12(2)^o$, $Z = 4$.

Introduction

The research in the area of new materials has rapidly expanded over the past 10 years. In particular, fields including ceramics,[1] liquid crystal,[2] organometallic and inorganic polymers,[3] dendrimers,[4] organic and inorganic conductors[5] and photoconductors.[6] Of particular interest, new materials for nonlinear optical properties,[7] microelectronic devices,[8] and diodes[9] have florished. Organic polymer chemistry remains a dominating field in comparison with the organometallic and inorganic counterpart, although the latter is receiving growing attention.[10]

Our research group recently reported the preparation and investigation of a unique type of polymer $\{[M(dmb)_2]Y\}_n$ (M

† A preliminary communication has been reported in: Harvey, P. D.; Fortin, D. *Coord. Chem. Rev.* **1998**, *171*, 351.

* To whom correspondence should be addressed: Telephone: (819) 821-8000 ext. 2005, (819) 821−7092. Fax:(819) 821-8017. E-mail: pharvey@courrier.usherb.ca.

‡ Laboratoire de diffraction des rayons-X.

(1) (a) For example, see: *Chemistry of High-Temperature Superconductors*; Nelson, D. L., Whittingham, M. S., George, T. F., Eds.; ACS Symposium Series 351; American Chemical Society: Washington, DC, 1987.

(2) Xu, B.; Swager, T. M. *J. Am. Chem. Soc.* **1993**, *115*, 1159. (b) Abe, A.; Kimura, N.; Tabata, S. *Macromolecules* **1991**, *24*, 6238.

(3) (a) Foucher, D. A.; Tang, B. Z.; Manners, I. *J. Am. Chem. Soc.* **1991**, *113*, 4044.

(4) (a) Worner, C.; Mülhaupt, R. *Angew. Chem., Int. Ed. Engl.* **1993**, *32*, 1306. (b) Brabander-van den Berg, E. M. M.; Meijer, E. W. *Angew. Chem., Int. Ed. Engl.* **1993**, *32*, 1308.

(5) (a) Haddon, R. C.; Hebard, A. F.; Rosseinsky, M. J.; Murphy, D. W.; Duclos, S. J.; Lyons, K. B.; Miller, B.; Rosamilia, J. M.; Fleming, R. M.; Kortan, A. R.; Glarum, S. H.; Maklija, A. V.; Muller, A. J.; Eick, R. H.; Zahurak, S. M.; Tycko, R.; Dabbagh, G.; Thiel, F. A. *Nature* **1991**, *350*, 320. (b) Jarrett, C. P.; Pichler, K.; Newbould, R.; Friend, R. H. *Synth. Met.* **1996**, *77*, 35. (c) *Low-Dimensional Conductors and Superconductors*; Jerome, D.; Caron, L. G., Eds.; Plenum Press: New York, 1986.

(6) (a) Köhler, A.; Wittmann, H. F.; Friend, R. H.; Khan, M. S.; Lewis, J. *Synth. Met.* **1994**, *67*, 245. (b) Lee, C. H.; Yu, G.; Moses, D.; Pakbaz, K.; Zhang, C.; Sariciftci, N. S.; Huger, A. J.; Wudl, F. *Phys. Rev. B* **1993**, *48*, 15425. (c) Janssen, R. A. J.; Christiaans, P. T.; Hare, C.; Nazario, M.; Sariciftci, N. S.; Huger, A. J.; Wudl, F. *J. Chem. Phys.* **1995**, *103*, 8840. (d) Shuai, Z.; Brédas, J. L.; Su, W. P. *Chem. Phys. Lett.* **1994**, *228*, 301. (e) Pakbaz, K.; Lee, C. H.; Huger, A. J.; Hagler, T. W.; McBranch, D. *Synth. Met.* **1994**, *64*, 295.

(7) (a) Truong, K. D.; Grenier, P.; Houde, D.; Bandrauk, A. D. *Chem. Phys. Lett.* **1992**, *196*, 180. (b) Truong, K. D.; Bandrauk, A. D.; Tran-Thi, T. H.; Grenier, P.; Houde, D.; Palacin, S. *Thin Solid Films* **1994**, *244*, 981. (c) Pollagi, T. P.; Stoner, T. C.; Dallinger, R. F.; Gilbert, T. M.; Hopkins, M. D. *J. Am. Chem.* **1991**, *113*, 703. (d) Pollagi, T. P.; Geib, S. J.; Hopkins, M. D. *J. Am. Chem. Soc.* **1994**, *116*, 6051.

(8) See, for example: Hickman, J. J.; Zou, C.; Ofer, D.; Harvey, P. D.; Wrighton, M. S.; Laibinis, P. E.; Bain, C. D.; Whitesides, G. M. *J. Am. Chem. Soc.* **1989**, *111*, 7271.

(9) (a) Burroughts, J. H.; Bradley, D. D. C.; Brown, A. R.; Marks, R. N.; Mackay; Friend, R. H.; Burns, P. L.; Holmes, A. B. *Nature* **1990**, *347*, 539. (b) Marks, R. N.; Bradley, D. D. C.; Jackson, R. W.; Burn, P. L.; Holmes, A. B. *Synth. Met.* **1993**, *55−57*, 4128. (c) Gustafsson, G.; Cao, Y.; Treacy, G. M.; Klavetter, F.; Colaneri, N.; Heeger, A. J. *Nature* **1992**, *357*, 477.

10.1021/ic990975o CCC: $19.00
Published on Web 06/06/2000

Chart 1

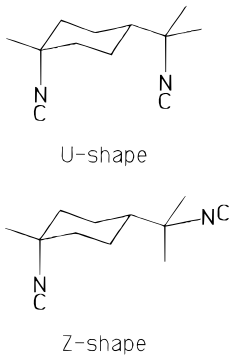

Chart 2

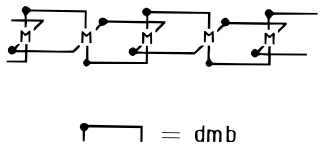

= Cu, Ag; Y = PF_6^-, BF_4^-, NO_3^-, ClO_4^-, $CH_3CO_2^-$).[11] The structure of these weakly soluble and electrically insulating materials consists of a series of metal atoms that are tetracoordinated by four dmb ligands via the isocyanide groups in a distorted tetrahedral fashion (drawings for dmb and the polymer are shown in Charts 1 and 2, respectively). These materials also exhibit glass transitions in the 40−100 °C range, and are strongly luminescent at 77 K both in the solid state and glassy solutions.[11] The preparation and X-ray diffraction analysis of a series of novel {[Ag(dmb)$_2$TCNQ}$_n$ materials were subsequently reported,[12] within which slow polymer isomerization in solution, along with $TCNQ^-$ counteranions dimerizations in the solid state, were observed. The isomerization occurs via a change in dmb conformation from the U-shape to the Z-shape (Chart 1). The ease with which the $TCNQ^-$ species dimerize encouraged us to seek further π-stacking in order to promote the formation of a linear π-stacked mixed valent $TCNQ_n^{x-}$ chain.

In this work we report the design and characterization of new semi- and photoconducting materials of the type {[M(dmb)$_2$]-TCNQ·xTCNQ°}$_n$ that do not lose their thermoplastic behavior. More particularly, above the glass transition the materials are still semiconducting. During the course of this study, one of the materials ({[Cu(dmb)$_2$TCNQ·1.5TCNQ}$_n$) was found to be photoconducting, and the design of a photocell of the type glass/SnO_2/polymer + acceptor/Al was accomplished.

Experimental Section

Material. The {[M(dmb)$_2$]Y}$_n$ polymers (M = Cu, Ag; Y = BF_4^-, ClO_4^-) and the "linear" {[Ag(dmb)$_2$]TCNQ·CH_2Cl_2}$_n$ material were prepared according to literature procedures.[11,12] The bridging ligand dmb,[13] electroacceptor TCNQ,[14] and LiTCNQ[14] salt were also synthesized according to reported procedures. The solvents used (CH_2Cl_2 (Aldrich), toluene, acetonitrile, tetrahydrofuran (THF; Fisher)) were purified according to procedures outlined in ref 15. The starting materials $AgClO_4$, $CuClO_4·6H_2O$, $AgBF_4$, and $Cu(BF_4)_2·H_2O$ were from Aldrich Chem. Co., and were used as received.

(a) {[Ag(dmb)$_2$]TCNQ·2THF}$_n$. A 0.978 g (1.701 mmol) sample of {[Ag(dmb)$_2$BF$_4$}$_n$ was dissolved in 100 mL of acetonitrile, which was then added to 50 mL of distilled water. The solution was stirred until the solution was clear, and 0.4 g (1.894 mmol) of LiTCNQ was then added. The resulting purple solution was stirred further for 5 h, and was subsequently evaporated under vacuum to dryness. The precipitate was then redissolved in CH_2Cl_2 and extracted with water. The solution was dried over K_2CO_3 overnight, and filtered. After complete evaporation, a dark green powder was obtained. Yield. 95%, T_f 181 °C, T_d 203 °C (according to TGA); FT-IR (KBr pellets) 2154 cm^{-1} (C≡N); ^{1}H NMR (CD_2Cl_2) 1.12−1.18 ppm (br, 36H) dmb, 1.8−2.4 (br, 4H)$TCNQ^-$; UV−vis (CH_3CN) 744 nm (structured), 420 nm (structured). No peak associated with BF_4^- was detected by IR. Single crystals suitable for X-ray crystallography were obtained from vapor diffusion of diethyl ether into THF solutions and the identity of the polymer was confirmed as {[Ag(dmb)$_2$]TCNQ·2THF}$_n$.

(b) Linear {[Cu(dmb)$_2$]TCNQ·0.25CH$_2$Cl$_2$}$_n$. The lesser crystalline polymer was prepared using a similar procedure to that reported for {[Ag(dmb)$_2$TCNQ·CH_2Cl_2}$_n$ except that the synthesis was adapted for Cu.[12] The {[Cu(dmb)$_2$BF$_4$}$_n$ used in this case was the *amorphous* material obtained from a stoichiometric reaction between dmb and [Cu^I-$(NCCH_3)_4$]BF_4 (2:1), according to a procedure reported in ref 11a. The more crystalline polymer was prepared the same way except that the *semicrystalline* {[Cu(dmb)$_2$BF$_4$}$_n$ was used. The latter was prepared from a direct reaction between dmb in excess and $Cu^{II}(BF_4)_2·xH_2O$, also according to a literature procedure.[11a] The general synthesis procedure was the same for both materials which will be referred as **1** and **2**, respectively, and is as follows. A 1 g (1.839 mmol) sample of {[Cu(dmb)$_2$]BF$_4$}$_n$ was dissolved in 200 mL of acetonitrile. The solution was then refluxed. After cooling this solution, 100 mL of an acetonitrile solution containing 0.4 (1.894 mmol) of LiTCNQ was then added. The solution was stirred for 8 h, prior to evaporating the solution to dryness. The purple precipitate was redissolved in 100 mL of CH_2Cl_2 and was extracted with water until complete disappearance of the blue coloration of the H_2O phase. The solution was dried over K_2CO_3, then was filtered. The remainder was then evaporated to dryness, and the product appeared as dark green brittle microcrystals. Yield 65−70%; (both **1** and **2**) T_d 240 °C (TGA); FTIR (Br pellets) 2153 cm^{-1} (C≡N); ^{1}H NMR (CD_2Cl_2) 1.2−1.8 ppm (br, 36H) dmb, 1.8−2.4 ppm (br, 4H) $TCNQ^-$. Anal. Calcd for $CuC_{36}H_{40}N_8·0.25CH_2Cl_2$: C, 65.09; H, 6.40; N, 16.61. Found: C, 65.05; H, 6.05; N, 16.75; UV−vis (CH_3CN) 744 nm (structured), 420 nm (structured). No peak associated with BF_4^- was detected by IR.

(c) {[Ag(dmb)$_2$]TCNQ·0.5TCNQ°·0.5 toluene}$_n$. A 0.389 g (0.5 mmol) sample of {[Ag(dmb)$_2$]TCNQ·CH_2Cl_2}$_n$ and 0.102 g (0.5 mmol) of TCNQ° were mixed in the solid state. This mixture was added to 100 mL of boiling acetonitrile until saturation was reached. To this warm solution, an equivalent volume of toluene was added, and the solution was heated to boiling again, promoting slow evaporation of acetonitrile. When the color of the solution turned yellow/green, the solution was filtered and kept at 90 °C in a water bath for several days. Black shiny crystals were obtained which exhibited needlelike shapes. Yield 73%, T_f 180 °C; FTIR 2181 cm^{-1}, 2153 cm^{-1} (ν(C≡N)). UV−vis (CH_3CN): 744 nm (structured), 420 nm (structured). The presence of strong and large peaks at 1430, 1382, 1362, and 1174 cm^{-1} in the IR spectra were observed and indicated the presence of π-stacking vibronic coupling. The identity of the product was made from X-ray crystallography, and indicated the presence of 0.5 toluene molecule per Ag.

(d) {[Ag(dmb)$_2$]TCNQ·TCNQ°}$_n$. A 0.692 g (1.00 mmol) sample of freshly prepared {Ag(dmb)$_2$TCNQ·CH_2Cl_2}$_n$ and 0.204 g (1.00 mmol) of TCNQ° were mixed in 100 mL of pyridine. Then the solution

(10) See for examples: (a) Begley, M. J.; Hubberstey, P.; Stroud, J. *J. Chem. Soc., Dalton Trans.* **1995**, 2323. (b) Erxleben, A.; Lippert, B. *J. Chem. Soc., Dalton Trans.* **1996**, 2329. (c) Black, J. R.; Champness, N. R.; Levason, W.; Reid, G. *J. Chem. Soc., Chem. Commun.* **1995**, 1277. (d) Feldman, J.; Calabrese, J. C. *Inorg. Chem.* **1994**, *33*, 5955.
(11) (a) Fortin, D.; Drouin, M.; Turcotte, M.; Harvey, P. D. *J. Am. Chem. Soc.* **1997**, *119*, 531. (b) Perreault, D.; Drouin, M.; Michel, A.; Harvey, P. D. *Inorg. Chem.* **1992**, *31*, 3688.
(12) Fortin, D.; Drouin, M.; Harvey, P. D. *J. Am. Chem. Soc.* **1998**, *120*, 5351.
(13) Weber, W. D.; Gokel, G. W.; Ugi, I. K. *Angew. Chem., Int. Ed. Engl.* **1972**, *11*, 530.
(14) Acker, D. S.; Hertler, W. R. *J. Am. Chem. Soc.* **1962**, *84*, 3370.
(15) (a) Perrin, D. D.; Armarego, W. L. F.; Perrin, D. R. *Purification of Laboratory Chemicals*; Pergamon: Oxford, U.K., 1966. (b) Gordon, A. J.; Ford, R. A. *The Chemist's Companion, a Handbook of Practical Data Techniques, and References*; Wiley: New York, 1972; p 436.

was refluxed for 20 min, cooled to room temperature, and was filtered. The bright black material was then precipitated out using CCl_4, then was filtered out. This method of preparation resulted in the best conducting material. Yield > 80%. Anal. Calcd for $AgC_{48}H_{44}N_{12}$: C, 64.29; H, 4.94; N, 18.74. Found: C, 64.22; H, 4.97; N, 18.01. The presence of 1 $TCNQ^-$ for 1 TCNQ° was readily confirmed by ^1H NMR, and UV−vis spectroscopy. Yield >80%, T_{dec} 175 °C. ^1H NMR (CD_2Cl_2): 1.12−1.18 ppm (br, 18H) dmb, 1.8−2.4 ppm (br, 4H) TCNQ. IR (Br): 2175 cm^{-1} (ν(N≡C)). Single crystals were obtained by vapor diffusion pyridine/CCl_4, but were found to be too small for crystallography analysis.

(e) {[Cu(dmb)$_2$]TCNQ·TCNQ°}$_n$. A 0.660 g (1.00 mmol) sample of {[Cu(dmb)$_2$]TCNQ·0.25 CH_2Cl_2}$_n$ and 0.204 g (1.00 mmol) of TCNQ° were mixed in 100 mL of pyridine. The solution was then refluxed for 20 min, cooled to room temperature, and then filtered. The black material was precipitated out using CCl_4, then filtered out. This method of preparation also led to the best conducting material. Yield >80%. The presence of 1 $TCNQ^-$ for 1 TCNQ° was readily confirmed by ^1H NMR, and UV−vis spectroscopy. Yield >85%, T_{dec} > 360 °C. Anal.: Calcd for $CuC_{48}H_{44}N_{12}$: C, 67.63; H, 5.20; N, 19.72. Found: C, 68.01; H, 5.25; N, 19.52. ^1H NMR (CD_2Cl_2): 1.12−1.18 ppm (br, 18H) dmb, 1.8−2.4 ppm (br, 4H) TCNQ. IR(Br): 2176 cm^{-1} (ν(N≡C)). UV−vis (CH_3CN) 744 (structured) and 394 nm (unstructured).

(f) {[Ag(dmb)$_2$]TCNQ·1.5TCNQ}$_n$. A 0.389 g (0.50 mmol) sample of freshly prepared {[Ag(dmb)$_2$]TCNQ·CH_2Cl_2}$_n$ (linear form), or 0.382 g (0.50 mmol) of {[Ag(dmb)$_2$]TCNQ·2THF}$_n$ was dissolved in 100 mL of a 50:50 v/v mixture of acetone: EtOH in the presence of excess TCNQ°. The mixture was refluxed and filtered, prior to being layered over a bed of solid TCNQ°. Olive-green crystals were readily obtained from slow evaporation of the solutions, and were suitable for X-ray crystallography analysis allowing clear identification of the new material. Yield >80%. T_{dec} <360 °C ^1H NMR (CD_2Cl_2): 1.12−1.18 ppm (br, 36H) dmb, 1.8−2.4 ppm (br, 10H) TCNQ. FT-IR (KBr): 2175 cm^{-1} (ν(N≡C)). UV−vis (CH_3CN) 744 (structured), 420 (structured), 394 nm (unstructured).

(g) {[Cu(dmb)$_2$]TCNQ·1.5TCNQ}$_n$. A 0.325 g (0.50 mmol) sample of {[Cu(dmb)$_2$]TCNQ·0.25 CH_2Cl_2}$_n$ was dissolved in 100 mL of a 50:50 v/v mixture of acetone: EtOH in the presence of excess TCNQ°. The mixture was then refluxed and filtered, prior being layered over a bed of solid TCNQ°. A olive-green solid was obtained from slow evaporation of the solution, but no crystal suitable for X-ray crystallography was obtained. Yield > 80%; T_m 206 °C. Anal. Calcd for $CuC_{54}H_{46}$: C, 67.94; H, 4.86; N, 20.54. Found: C, 67.87; H, 4.92; N, 20.31. ^1H NMR (CD_2Cl_2): 1.12−1.18 ppm (br, 36H) dmb, 1.8−2.4 ppm (br, 10H) TCNQ; FT-IR (KBr): 2176 cm^{-1} (ν(N≡C)). UV−vis (CH_3CN) 744 (structured), 420 (structured), 394 nm (unstructured).

(h) {[Ag(dmb)$_2$]DCTC}$_n$ (DCTC = α,α-Dicyano-*p*-toluolylcyanate). A 0.100 g (0.125 mmol) sample of {[Ag(dmb)$_2$]TCNQ·CH_2Cl_2}$_n$ (purple) was broad band irradiated for several days in the solid state with a Canrad-Hanovia 450 W lamp at a distance of 30 cm. Orange-brown crystals suitable for X-ray crystallography were obtained from slow vapor diffusion of diethyl ether into a CH_2Cl_2 solution, and allowed the identification of the photoproduct. Yield >80%; FT-IR (Br): 2175 br (ν(N≡)), 1645 cm^{-1} (ν(C≡O)). UV−vis (CH_3CN): 480 nm.

(i) 13,13,14,14-Tetracyano-5, 12-naphthacenequinodimethane, TCNN. This acceptor molecule was prepared according to a modified procedure reported by Nazario et al.[16] since the predicted yield was never obtained (~55%). A 1.000 g (3.873 mmol) sample of 5,12-naphtacenequinone[17] was dissolved in 400 mL of toluene, 75 mL of 2-butanol, and 30 mL (2.099 mol) of malonitrile, which contained 0.05 g of β-alanine. This solution was refluxed for 2 h and dried using a Dean−Stark apparatus operating under N_2. Then 2 mL of $TiCl_4$ was added, and the solution was further refluxed for 48 h. Subsequently 400 mL of toluene was added to the cooled solution, then the solution was filtered and evaporated until a brown oily residue was obtained. This residue was $CH_2(CN)_2$. To this oil, was added 150 mL of MeOH, and the mixture was stirred vigorously. Then the yellow product was filtered and recrystallized 3 times in hot toluene. The product appeared as long yellow needles. Yield ~30%. T_f > 320 °C. ^1H NMR ($CDCl_3$): 8.69 ppm (s, 2H), 8.25−8.23 ppm (m, 2H), 8.03−8.01 ppm (m, 2H), 7.75−7.72 ppm (m, 4H). FT-IR (Br): 2231 cm^{-1} (ν(C≡N)). UV−vis ($CHCl_3$): λ_{max} 262, 302, 326, 425 nm. MS: *m*/*e* 354 M^+.

X-ray Structure Determination. For all compounds, the data collections were made with an Enraf-Nonius diffractometer using copper monochromatic X-ray radiation (Cu Kα = 1.54184 Å). The measurements were performed at 173 K for all compounds except for {Ag(dmb)$_2$DCTC}$_n$ which was carried out at room temperature. The DIFRAC program was used for indexation, crystal centering, and data collection. The data reduction was done using the DATRDZ program, structure solving performed via the direct methods using the program SOLVER, both included in the NRCVAC[18] program. The refinement was carried out using the SHELXL-97 program.

{[Ag(dmb)$_2$]TCNQ·2THF}$_n$. The unit cell dimensions were obtained from 24 reflections, and were a = 13.5501(10), b = 9.9045(10), c = 32.564(2) Å, and β = 91.130(10)° with a monoclinic space group $P2_1/c$. Two standard reflections were monitored every 60 min, and did not decrease significantly. At convergence, R = 0.0589, wR2 = 0.1550, and S = 1.056 for 5384 observed reflections. The positive and negative residuals around the silver atoms (ΔF) were +0.939 and −1.341 e/Å^3. For all atoms, except for the H atoms, the refinement was performed anisotropically. The H atoms were geometrically placed and were not refined. One of the dmb ligands was disordered and was refined using the constraints named SAME and SADI from the program SHELXL-97.[19] At convergence the occupancy ratio was 0.736(5)/0.264(5). Only the major occupancy was used for the drawings. The maximum value for Δ/σ after refinement was 0.0003.

{[Ag(dmb)$_2$]TCNQ·1.5TCNQ°}$_n$. The unit cell parameters were a = 25.830(11), b = 9.680(2), c = 42.183(19) Å, and β = 104.87(4)° for a monoclnic space group $C2/c$. Two standard reflections were monitored every 60 min and did not decrease significantly with time. At convergence, the residuals were R = 0.0700, wR2 = 0.1721, and S = 0.948 for 7540 observed reflections. The positive and negative residuals around the silver atoms (ΔF) were +1.612 and −1.632 e/Å^3. Except for the H atoms, the other atoms were refined anisotropically. The positions of H atoms were calculated, not refined. The dmb ligands were disordered and were refined with the constraints SAME and SADI from the program SHELXL-97. The occupancy ratio at convergence were 0.628(6)/0.372(6) and 0.530(6)/0.470(6). Only the major conformations were used for the drawings. The maximum Δ/σ value after refinement was 0.0001.

{[Ag(dmb)$_2$]TCNQ·0.5TCNQ°·0.5 toluene}$_n$. The unit cell parameters were a = 14.3669(19), b = 9.1659(3), c = 34.012(3) Å, and β = 92.140(8)°, for a monoclinic system, space group $P2_1/c$. Two standard reflections were monitored every 60 min and did not significantly decrease with time. The positive and negative residuals around (ΔF) were +0.516 and −0.515 eÅ^{-3}. All nondisordered atoms were refined anisotropically. The dmb ligands are disordered and were refined with the constrainsts SAME and SADI available in the SHELXL-97 program. The occupancy ratio were at convergence 0.750(5)/0.250(5) and 0.798(5)/0.202(5). Only the major occupancy atoms were used for the drawings. The maximum Δ/σ value was 0.072 in the last cycle of refinement.

{[Ag(dmb)$_2$]DCTC}$_n$. The unit cell parameters were a = 26.273(3), b = 9.730(3), c = 31.526(3) Å, and β = 112.12(2)°, for a monoclinic system, space group = $P2_1/a$. Two standard reflections were monitored every 60 min and did not decreased significantly with time. At convergence, the residuals were R = 0.1357, wR2 = 0.3015, and S = 1.480 for 4535 observed reflections. The positive and negative residuals around the silver atoms (ΔF) were +1.917 and −0.993 e/Å^3. Except for the H atoms, the other atoms were refined anisotropically. The positions of the H atoms were calculated, not refined. The maximum Δ/σ value was 0.021 after refinement.

Apparatus. The FT-IR spectra were obtained using a Bomem Michelson 100 spectrometer, and were analyzed using the program

(16) Nazario, M.; Behnish, R.; Hanack, M. *J. Org. Chem.* **1989**, *54*, 2563.
(17) Serpand, B.; Lepage, Y. *Bull. Soc. Chim. Fr.* **1977**, 539.
(18) Gabe, E. J.; Lepage, Y.; Charland, J. P.; Lee, F. L.; White, P. S. *J. Appl. Crystallogr.* **1989**, *22*, 384.
(19) Sheldrick, G. SHELXL-97, Institüt Anorg. Chemie, Tammanstr. 4, 037077, Göttingen, Germany, 1997.

Spectra Calc. W2.20. The NMR spectra were measured on a Bruker AC-300 instrument. The UV−visible spectra were acquired on a Hewlett-Packard 8452A (diode array) at 298 K. The luminescence spectra were obtained on a SPEX Fluorolog II double monochromator. The emission lifetime measurements were performed using this same instrument coupled with a SPEX 1934D phosphorimeter. The TGA analyses were performed using a Perkin-Elmer TGA7 apparatus operating between 30 and 300 °C scanning at a rate of 10°/min under Ar atmosphere. The glass transition temperatures (T_g) were determined using a Perkin-Elmer 5A DSC7 apparatus, equipped with a thermal control analyzer 5B TAC 7/DS. The temperature calibrations were done with water and metallic indium as standards. The accuracy is ±0.1 °C and ±0.1%. The sample weights ranged from 5 to 10 mg, and the scan rate was adjusted at 20.0°/min. The X-ray powder diffraction patterns were acquired on a Rigaku/USA inc apparatus equipped with a copper source operating at 40 kV and 30 mA, in continuous standard, scans $2\theta/\theta$-reflection of 1°/min. The sample support was a standard aluminum support, and the slits were placed in positions $^1/_2$ SS and $^1/_2$ SD at the source and detector, respectively. The X-ray powder diffraction patterns were analyzed using the program TREOR90.[20] The elemental analysis (C,H,N) were performed at the Université de Montréal.

Conductivity and Photoconductivity Measurements. The conductivity measurements were performed on an homemade four-point probe apparatus designed according to S. M. Sze in ref 21. The samples were pressed pellets of 1.13 cm^2 surfaces. The potentials were measured with standard voltmeter Keithley 177 microvolt DMM, and the applied current was generated with a TRYGON model HH32-1.5 Systron-Donner Corp. source operating at 1.5A between 0 and 32 V. The precision was ±0.1%. For measurements as a function of temperature, the device was placed inside an oven with a variable temperature controller (±0.5 °C). The stabilization of the temperature took between 10 and 15 min prior to measurements. The photoconductivity measurements were performed on a modified version of the four-point probe apparatus. Instead the photoconductivity was measured by direct measurements of the current at constant potential, which was directly proportional to the conductivity increase according to $I = V\sigma$. The samples and electrode system were placed inside a black box 15 cm away from a 450 W mercury lamp from ACE GLASS Canrad-Hanovia. The lamp was water jacketed to ensure that no heat hit the samples. The air inside the box was also exchanged using a small fan. The temperature did not change during the measurements and was 20 °C (293 K).

Photovoltaic Cells. The cells were built by deposition of films on top of a conducting glass in the following order: glass, SnO_2, {[Cu(dmb)$_2$]TCNQ·TCNQ°}$_n$·acceptor, Al. The glass−SnO_2 substrate was obtained from Associates Estrel (Toledo, OH) and exhibited a resistivity of 8 Ω cm^2 and a transmittance of 80% in the visible region. The polymer film was obtained by depositing onto the glass-SnO_2 substrate, drop-by-drop, a saturated pyridine solution of {[Cu(dmb)$_2$]TCNQ·TCNQ°}$_n$ and acceptor (TCNQ, TCNN, or C_{60}), with a 1:0.5 molar ratio (polymer/acceptor) at 100−110 °C inside a preheated oven. This procedure was performed until dryness. This temperature is above the T_g of the polymeric material and ensured a better film formation. The thickness of the films was around 5 μm on average. Nail polish was applied on the uncovered portion and dried under vacuum. An Al film was vapor deposited using a homemade apparatus from Professor Hugues Ménard's laboratory (U. de Sherbrooke). An Al foil was wrapped around a W wire (R. D. Matlis Co. model F-15) which was heated under a vacuum of 1.5×10^{-5} Torr. The Al film formation was stopped until an opaque layer was obtained. Part of the Al film at the cell cover was mechanically removed, and the nail polish was washed with acetone, to provide electric contacts with the SnO_2 surface (positive electric contact), and Al surface (negative electric contact).

Osmometric Pressure Measurements. The osmometric pressure measurements for the evaluation of the average molecular weight in number (M_n) for the {[Cu(dmb)$_2$]BF$_4$}$_n$ polymers (**1** and **2**),[11a] were performed on a 4100 Colloid Osmometer from Werscor Inc. The ultrafiltration membranes were 43 mm diameter DIAFLO 10kD type-YM membranes from Amicon Inc. (lot: AJA403) which were stable even in acetonitrile solutions. The calibration was made with an AC-010 water manometer from Wescor Inc. allowing the conversion of mmHg into cm of H_2O pressure. Data collection was performed using a PC, a homemade program written in GW BASIC, and a DAS8 acquisition card from Megabyte. The data analysis was performed using Quattro Pro. The solutions were from 1% to 7% concentration where 1% = 1 g of polymer/100 mL of solution.

Results and Discussion

1. Preparation and Characterization. The preparation of the electrically insulating {[M(dmb)$_2$]TCNQ·solvate}$_n$ polymers (M = Cu, solvate = 0.25 CH_2Cl_2; M = Ag, solvate = 2THF) is easily achieved in good yields from the counteranionic methathesis of the corresponding {[M(dmb)$_2$Y}$_n$ starting materials (Y = BF_4^- or ClO_4^-). X-ray crystallography (Figure 1, Chart 3, and Tables 1 and 2) for {[Ag(dmb)$_2$]TCNQ·2THF}$_n$ reveals

Chart 3

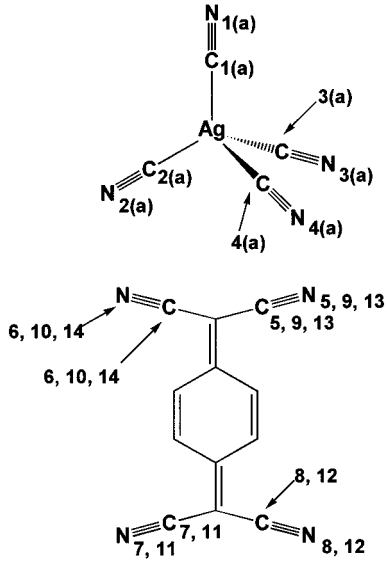

the expected {Ag(dmb)$_2^+$}$_n$ polymeric structure as described above where the Ag^+ metals are tetracoordinated by four dmb bridging ligands forming a zigzag chain. In this case, the Ag···Ag separations is 5.2829(6) Å, significantly longer than that observed for {[Ag(dmb)$_2$]TCNQ·CH_2Cl_2}$_n$ (5.065(3) Å).[12] Literature comparison for species where all dmb ligands adopt the U-shape conformation (Table 3) indicates that the former Ag···Ag separation is also the longest one in the {[Ag(dmb)$_2^+$]}$_n$ series. These comparisons indicate that the polymer backbone exhibits some degree of flexibility, despite the apparent "rigid rod" nature of the polymers,[11] and the presence of intramolecular dmb-dmb steric hindrance. The Ag_3 angle for this polymer is also ~140°, favorably comparing with most {[Ag(dmb)$_2^+$]}$_n$ materials. In direct relevance to this work, the solid-state

(20) The indexation analysis was performed using the commercially avaialble program TREOR90 from P.-E. Werner, Department of Structural Chemistry, Arrhenius Laboratory, University of Stockholm, S-106 91 Stockholm, Sweden. Explanations of the principles of the techniques can be found in the following references (a) Werner, P.-E. *Z. Kristallogr.* **1964**, *120*, 375. (b) Werner, P.-E.; Erikson, L.; Westdahl, M. *J. Appl. Crystallogr.* **1985**, *18*, 367. (c) Werner, P.-E. *Ark. Kemi* **1969**, *31*, 513. The criteria for reasonable solutions were as follows: (1) all strong scattering peaks must be indexed (I(rel.) > 40%), (2) most peaks if not all, must be indexed (I(rel.) >15%), 3) the *a*, *b*, and *c* parameters must be greater than 9 Å based upon literature and this work's data for {[Ag(dmb)$_2$]Y}$_n$ polymers,[11,12] and (4) unit cell angles should be between 75 and 120°, also based upon known data. Under these conditions, only a limited number of reasonable solutions are obtained, but no secure assignment can be provided in this work.

(21) Sze, S. M. *Physics of Semiconductors*, 2nd ed. John Wiley: Toronto, Canada, 1981; pp 30−32.

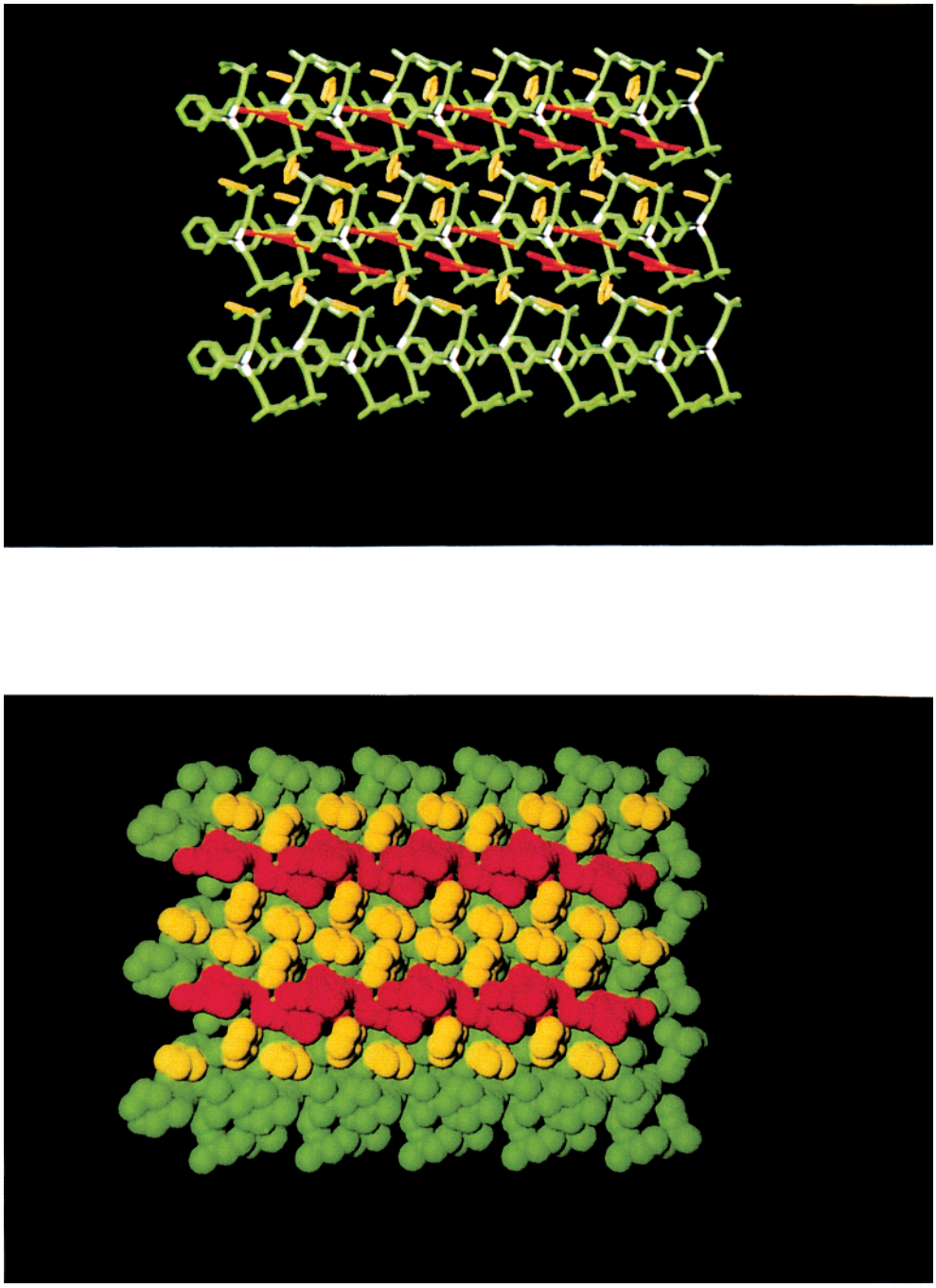

Figure 1. X-ray structure of $\{[Ag(dmb)_2]TCNQ\cdot 2THF\}_n$. Green = $\{Ag(dmb)_2^+\}$ (*n* chains: red = $TCNQ^-$; yellow = THF). Top = stick model; bottom = space-filling model.

structure for $\{[Ag(dmb)_2]TCNQ\cdot 2THF\}_n$ also reveals the presence of dimeric $TCNQ_2^{2-}$ species, consistent with our previous observations for other polymers.[12] In this case the interplanar $TCNQ^-\cdots TCNQ^-$ separation (3.24(4) Å) is somewhat shorter than that of the sum of the van der Waals radii for C (2 × 1.70 Å), the values found in the $\{[Ag(dmb)_2]TCNQ\cdot solvate\}_n$ polymeric isomers (3.346, 3.436, and 3.312 Å),[12] and the data reported for other dimer or trimer species (see for instance data for $[Pd(CNCH_3)_4](TCNQ)_4$ (3.29 and 3.36 Å),[22] $[Fe_2(\eta_5\text{-}C_5H_5)_2(\mu\text{-}CO)_2((C_6H_5)_2PN(C_2H_5)P(C_6H_5)_2)](TCNQ)_3$ (3.24 and 3.39 Å),[23] $((H_7C_3)_2NH)(TCNQ)_2$ (3.20 and 3.30 Å),[24] and $[C(C_6Me_6)Fe(\eta^5\text{-}C_5H_5)](TCNQ)_2$ (3.35 and 3.37 Å)[25]). In the TCNQ° crystal, this distance is also shorter (3.45 Å).[26]

The interesting feature is that the 3-D structure consists of a layered construction (Figure 1), where the $\{Ag(dmb)_2^+\}_n$ "sticks" stack side-by-side to form a cationic layer, and the $TCNQ^-$ and 2THF's crystallize perpendicularly to this first layer to form a new layer. Such a feature is new in the $\{[Ag(dmb)_2]Y\}_n$ chemistry.[11,12] The role of the THF solvation molecules clearly appears to be the filling empty spaces in the solid-

(22) Goldberg, S. Z.; Eisenberg, R.; Miller, J. S.; Epstein, A. J. *J. Am. Chem. Soc.* **1976**, *98*, 5173.
(23) Bell, S. E.; Field, J. S.; Haines, R. J. *J. Chem. Soc., Chem. Commun.* **1991**, 489.
(24) Truong, K. D.; Pepin, C.; Bandrauk, A. D.; Drouin, M.; Michel, A.; Banville, M. *Can. J. Chem.* **1991**, *69*, 1804.
(25) Lequan, R.-M.; Lequan, M.; Jaouen, G.; Ouahab, L.; Batail, P.; Padiou, J.; Sutherland, R. G. *J. Chem. Soc., Chem. Commun.* **1985**, 116.
(26) Long, R. E.; Sparks, R. A.; Trueblood, K. R. *Acta Crystallogr.* **1965**, *18*, 932.

Table 1. Crystallographic Data

	{[Ag(dmb)$_2$]TCNQ·2THF}$_n$	{[Ag(dmb)$_2$]TCNQ·0.5TCNQ·0.5toluene}$_n$	{[Ag(dmb)$_2$]TCNQ·1.5TCNQ}$_n$	{[Ag$_2$(dmb)$_4$]DCTC$_2$}$_n$
fw	836.41	840.80	998.92	1364.50
space group	$P2_1/c$	$P2_1/c$	$C2/c$	$P2_1/a$
a, Å	13.5501(10)	14.3669(19)	25.830(11)	26.273(3)
b, Å	9.9045(10)	9.1659(3)	9.680(2)	9.730(3)
c, Å	32.564(2)	34.012(3)	42.183(19)	31.526(3)
β, deg	91.130(10)	92.140(8)	104.87(4)	112.12(2)
V, Å^3	4369.5(6)	4475.8(7)	10194(7)	7466(3)
Z	4	4	8	4
T, °C	−100	−100	−100	20
λ(Kα_{ax}), Å	1.540 60	1.540 60	1.540 60	1.540 60
ρ_{cal}, g/cm^3	1.272	1.247	1.302	1.215
μ, cm^{-1}	40.41	39.29	35.71	44.53
R1[a]	0.0589	0.0563	0.0700	0.1357
wR2[b]	0.1550	0.1480	0.1721	0.3015

[a] $R1 = \Sigma||F_o|F_c||/\Sigma|F_o|$. [b] $wR2 = \{\Sigma[w(F_o^2 - F_c^2)^2]/\Sigma[w(F_o^2)^2]\}^{1/2}$.

Table 2. Selected Bond Distances and Angles[a]

	{[Ag(dmb)$_2$]TCNQ·2THF}$_n$	{[Ag(dmb)$_2$]0.5TCNQ°·0.5 toluene}$_n$	{[Ag(dmb)$_2$]TCNQ·1.5TCNQ°}$_n$	{[Ag(dmb)$_2$]DCTC}$_n$	
		Bond Distances/Å			
AgC_1, Ag_aC_{1a}	2.207(8)	2.249(11)	2.209(10)	1.91(4)	1.98(4)
AgC_2, Ag_aC_{2a}	2.227(8)	2.219(11)	2.231(9)	2.23(3)	2.19(4)
AgC_3, Ag_aC_{3a}	2.197(7)	2.181(10)	2.240(9)	2.25(3)	2.20(3)
AgC_4, Ag_aC_{4a}	2.228(7)	2.217(10)	2.214(8)	2.23(4)	2.01(5)
average	2.215	2.217	2.224	2.13	
C_1N_1, $C_{1a}N_{1a}$	1.123(9)	1.112(11)	1.138(11)	1.25(3)	1.22(3)
C_2N_2, $C_{2a}N_{2a}$	1.142(10)	1.159(10)	1.140(10)	1.13(3)	1.18(3)
C_3N_3, $C_{3a}N_{3a}$	1.149(8)	1.154(10)	1.125(10)	1.12(3)	1.08(3)
C_4N_4, $C_{4a}N_{4a}$	1.137(8)	1.147(10)	1.148(10)	1.15(3)	1.26(4)
average	1.138	1.143	1.138	1.17	
C_5N_5	1.152(10)	1.148(12)	1.149(11)	1.10(5)	
C_6N_6	1.155(10)	1.110(13)	1.146(11)	1.18(4)	
C_7N_7	1.141(11)	1.143(16)	1.163(12)	1.10(4)	
C_8N_8	1.137(10)	1.123(13)	1.155(12)		
C_9N_9		1.138(10)	1.160(11)		
$C_{10}N_{10}$		1.130(13)	1.156(11)		
$C_{11}N_{11}$			1.157(11)		
$C_{12}N_{12}$			1.156(11)		
$C_{13}N_{13}$			1.138(11)		
$C_{14}N_{14}$			1.131(12)		
average	1.146	1.132	1.151	1.13	
		Bond Angles/deg			
AgC_1N_1, $Ag_aC_{1a}N_{1a}$	172.7(6)	174.2(8)	171.9(8)	178(3)	169(3)
AgC_2N_2, $Ag_aC_{2a}N_{2a}$	167.6(6)	161.3(10)	168.0(8)	168(3)	169(3)
AgC_3N_3, $Ag_aC_{3a}N_{3a}$	172.1(6)	172.3(8)	167.9(8)	161(3)	163(3)
AgC_4N_4, $Ag_4C_{4a}N_{4a}$	164.6(6)	162.3(9)	169.8(8)	161(3)	167(4)
average	169.3	167.5	169.4	167	
C_1AgC_3, $C_{1a}Ag_aC_{3a}$	112.1(3)	104.0(3)	108.3(4)	99.3(14)	102.9(13)
C_1AgC_4, $C_{1a}Ag_aC_{4a}$	106.9(3)	108.8(3)	97.1(3)	105.9(12)	105.1(15)
C_1AgC_2, $C_{1a}Ag_aC_{2a}$	120.1(3)	120.7(4)	122.5(4)	125.6(14)	125.0(14)
C_2AgC_4, $C_{2a}Ag_aC_{4a}$	92.6(3)	93.8(4)	108.1(3)	105.9(12)	107.7(14)
C_2AgC_3, $C_{2a}Ag_aC_{3a}$	105.4(3)	106.7(4)	100.9(3)	105.0(11)	99.5(12)
C_3AgC_4, $C_{3a}Ag_aC_{4a}$	119.0(3)	124.0(4)	121.6(3)	117.8(13)	118.6(16)

[a] Atom numberings refer to Chart 3. Labelings C_1, C_{1a}, etc. apply only to {[Ag(dmb)$_2$] DCTC}$_n$ where two different Ag(dmb)$_2$ units are found.

state structure, in a way that the $(TCNQ)_2^{2-}$ dimers and 4THF molecules are placed in an alternative fashion describing a linear chain. The interplanar distance between two $(TCNQ)_2^{2-}$ groups is 10.195 Å, leaving enough space to place four THF molecules within the "hole". The THF molecules stack forming a windmill structure, but the centers of the THF's do not define a plane, but rather a stair shaped structure. The angle between the polymeric backbone and the $(TCNQ)_2^{2-}$/4THF chain is ∼55°.

Two different starting {[Cu(dmb)$_2$]BF$_4$}$_n$ materials are used for the preparation of the $TCNQ^-$ derivatives. These materials are the amorphous (**1**) and semicrystalline polymers (**2**). The molecular weight-averaged in number (M_n) is obtained for these starting materials from osmotic pressure measurements and are as follows: semicrystalline (**2**), ∼133 000, and amorphous (**1**), ∼140 000. For the remainder of this work, it is assumed that M_n is not a function of the counteranion and that M_n remains constant. X-ray powder diffraction patterns established that both materials are semicrystalline, with the exception that the polymer prepared from the amorphous starting material **1** is less crystalline than the other.

The preparation of the {[M(dmb)$_2$]TCNQ·xTCNQ°}$_n$ materials (M = Ag, Cu, x = 1; M = Ag, x = 0.5 (and solvate = 0.5 toluene)), is easily achieved from appropriate stoichiometric additions of TCNQ° to freshly prepared corresponding {[M(dmb)$_2$]TCNQ·solvate}$_n$ polymers. The X-ray structure for {[Ag(dmb)$_2$]TCNQ·0.5TCNQ·0.5 toluene}$_n$ reveals the presence

Table 3. Structural Comparison of the Various $\{Ag(dmb)_2^+\}_n$ Polymers[a]

polymers	D(Ag···Ag)/Å	∠AgAgAg/deg	ref
$\{[Ag(dmb)_2]TCNQ\cdot 2THF\}_n$	5.2829(6)	139.25(2)	this work
$\{[Ag(dmb)_2]TCNQ\cdot 1.5TCNQ°\}_n$	5.2787(11)	132.96(3)	this work
$\{[Ag(dmb)_2]DCTC\}_n$	5.203(6)	139.85(7)	this work
	5.156(6)	139.85(7)	
$\{[Ag(dmb)_2]NO_3\cdot 0.70H_2O\}_n$	5.1884(6)	139.88(1)	11a
$\{[Ag(dmb)_2]TCNQ\cdot CH_2Cl_2\}_n$	5.065(3)	140.364(10)	12
$\{[Ag(dmb)_2]PF_6\}_n$	4.964(1)	139.15(4)	11b
$\{[Ag(dmb)_2]BF_4\}_n$	4.9557(9)	140.46(2)	11a
$\{[Ag(dmb)_2]ClO_4\}_n$	4.9496(1)	139.57(2)	11a
$\{[Ag(dmb)_2]TCNQ\cdot 0.5TCNQ\cdot 0.5C_7H_8\}_n$	4.8816(4)	139.71(3)	this work

[a] Only examples where both dmb's exhibit the same U-shape conformation are listed. See ref 12 for other examples, where the dmb's do not adopt the same conformation within the polymer backbone.

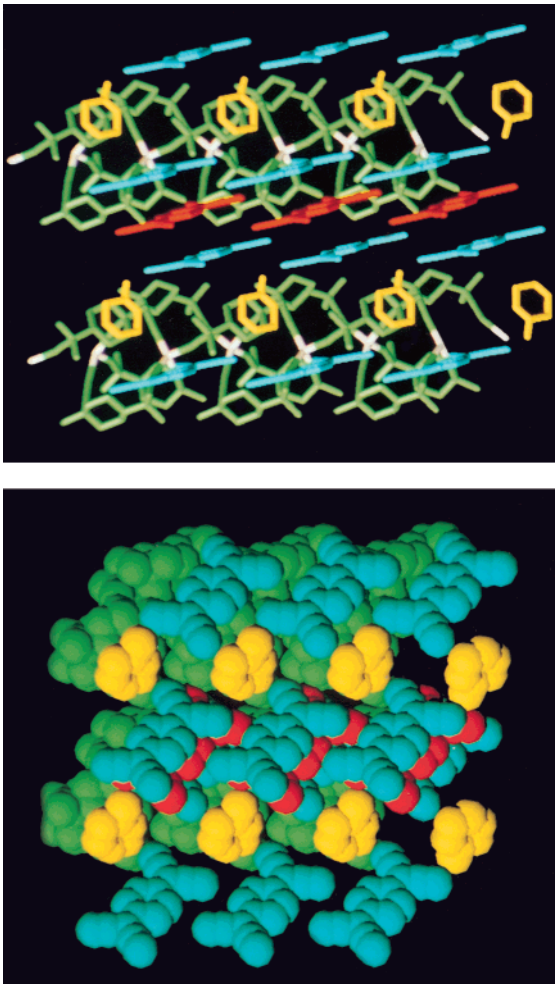

Figure 2. X-ray structure of $\{[Ag(dmb)_2]TCNQ\cdot 0.5TCNQ°\cdot$ 0.5 toluene$\}_n$. Green = $\{[Ag(dmb)_2^+\}_n$ chains; red and blue = TCNQ; yellow = toluene. Top = stick model; bottom = space-filling model.

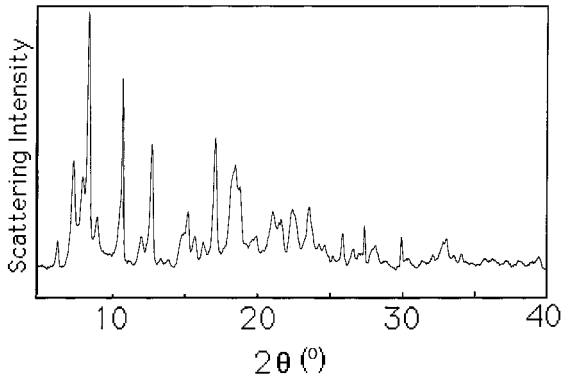

Figure 3. X-ray powder diffraction pattern for the $\{[Ag(dmb)_2]TCNQ\cdot TCNQ°\}_n$ polymer.

Table 4. Comparison of the Electric Conductivities for the $\{[M(dmb)_2]TCNQ\cdot TCNQ°\}_n$ Materials[a]

compounds	σ/S cm^{-1}	M_n
$\{[Ag(dmb)_2]TCNQ\cdot TCNQ°\}_n$	2.40×10^{-2}	<10 000
$\{[Ag(dmb)_2]TCNQ\cdot 1.5TCNQ°\}_n$	2.86×10^{-2}	<10 000
$\{[Cu(dmb)_2]TCNQ\cdot TCNQ°\}_n$ (**1**)	3.07×10^{-4}	∼133 000
$\{[Cu(dmb)_2]TCNQ\cdot TCNQ°\}_n$ (**2**)	4.84×10^{-4}	∼140 000
$\{[Cu(dmb)_2]TCNQ\cdot 1.5TCNQ°\}_n$ (**1**)	4.34×10^{-4}	∼133 000
$\{[Cu(dmb)_2]TCNQ\cdot 1.5TCNQ°\}_n$ (**2**)	6.06×10^{-4}	∼140 000

[a] Pressed pellets. **1** and **2** refer to the lesser and more crystalline materials, respectively, as described in the Experimental Section.

of slightly spaced $\{Ag(dmb)_2^+\}_n$ chains parallelly stacked, along with mixed-valence $(TCNQ)_3^{2-}$ trimers and toluene molecules. The $(TCNQ)_3^{2-}$ species are placed somewhat between the cationic polymers, and crystallize rather side-by-side (Figure 2). This absence of an infinite chain of mixed-valence π-stacked $TCNQ^{x-}$ in the solid is consistent with the insulating properties of this material. There is no obvious chain of the type $(TCNQ)_3^{2-}$···toluene··· etc., in this case. The interplanar distances within the $(TCNQ)_3^{2-}$ species are 3.32(4) Å, and compare favorably to that of other literature examples as listed above.[22−25]

The role of toluene seems unclear at first, with respect to the π-stacked $TCNQ^{x-}$ chain. The Ag···Ag separation is 4.8816(4) Å and is the shortest distance ever measured for such polymeric systems. With an Ag_3 angle of 139.71(3)°, the Ag···Ag distance in the zigzag structure from tip-to-tip is 9.1659(4) Å. Such a distance would then leave 3.057 Å only as interplanar between the $TCNQ^{-2/3}$, if the TCNQ chain was to stack parallelly to the polymer backbone. This value falls significantly short in comparison with good semiconducting materials based upon TCNQ π-stacking (∼3.17 Å).[27] This geometric constraint suggests that the absence of this infinite TCNQ chain is apparently not due to the toluene crystallization molecule, but rather to a mismatch in Ag···Ag and appropriate interplanar TCNQ's distances.

No crystal suitable for X-ray structure determination was obtained for the electrically semiconducting $\{[Ag(dmb)_2]TCNQ\cdot TCNQ°\}_n$ materials. The 1:1 $TCNQ^-/TCNQ°$ molar ratio has been unambiguously established from chemical analysis and several spectroscopic methods. Indeed using Beer−Lambert's law, and the comparison of the absorptivities of the electronic bands associated with $TCNQ^-$ (∼780 nm) and TCNQ° (∼480 nm) for crystallographically characterized materials in this work ($\{[Ag(dmb)_2]TCNQ\cdot xTCNQ\}_n$ where $x = 0.5$ and 1.5 (structure discussed below)), the stoichiometry is readily established at 1:1. The integration of the ^1H NMR signals associated with $TCNQ^-$ and TCNQ° also confirms this ratio, despite the

(27) Endees, H. *Angew. Chem., Int. Ed. Engl.* **1984**, *23*, 999.

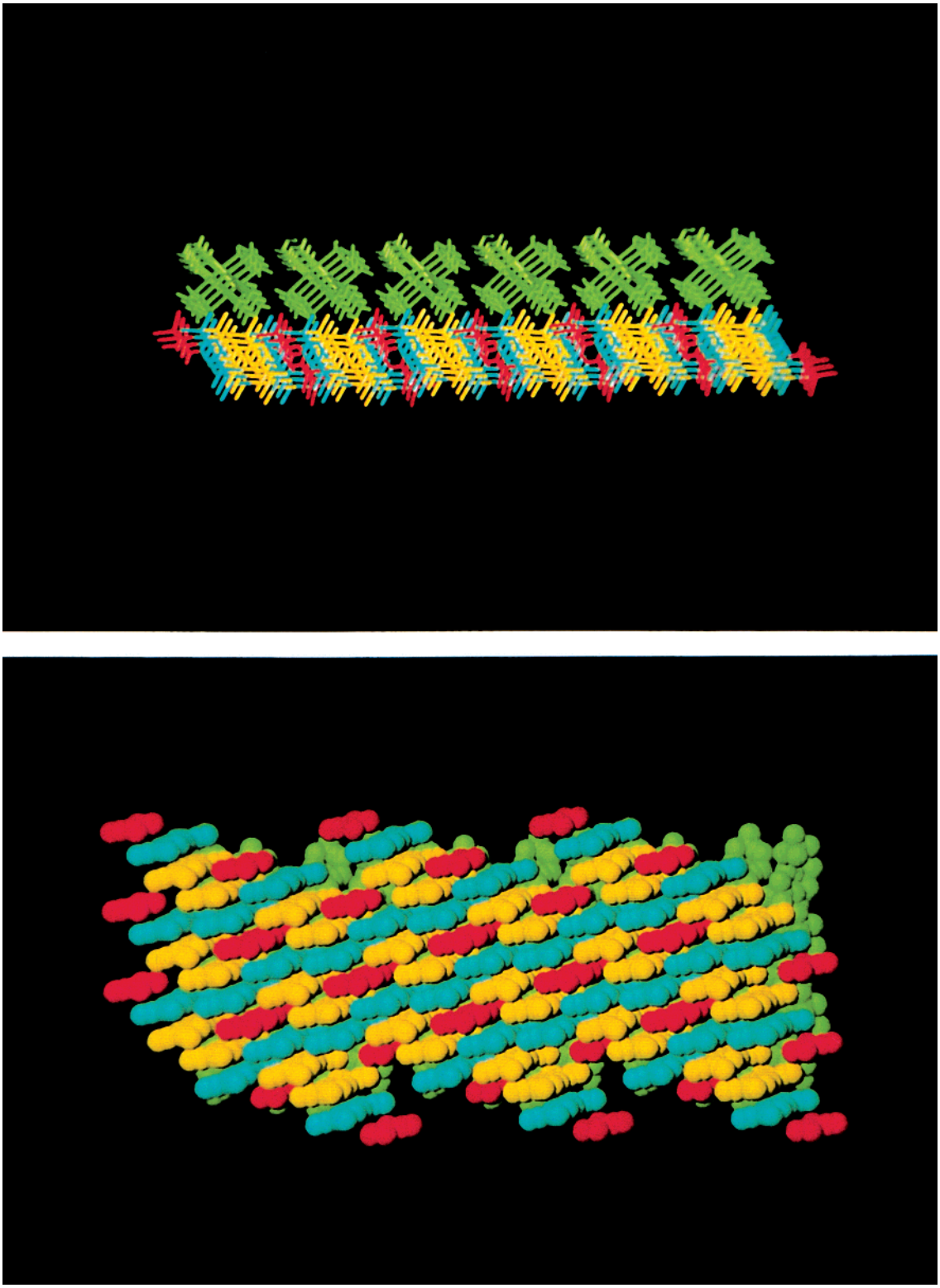

Figure 4. X-ray structure of {Ag(dmb)$_2$]TCNQ·1.5TCNQ°}$_n$. Green = {Ag(dmb)$_2^+$}$_n$ chains; red, blue, and yellow = TCNQ. Top = stick model (side view); bottom = space-filling model (down view).

presence of paramagnetic species. The X-ray diffraction patterns (Figure 3) indicate that this material is crystalline, and a reasonable indexation solution is obtained (monoclinic, a = 29.36 Å, b = 10.99 Å, c = 13.81 Å, β = 96.5°, V = 4428 Å^3, for 18 indexed peaks; Supporting Information).

In the absence of suitable crystal for X-ray diffraction analysis, the identification and characterization of the {[Cu(dmb)$_2$]TCNQ·TCNQ°}$_n$ polymers (**1** and **2**) proceeded similarly to that described above. The electric conductivities which are on the order of (3−5) × 10^{-4} S cm^{-1} for these materials (Table 4), and 2.40 × 10^{-2} S cm^{-1} for {[Ag(dmb)$_2$]TCNQ·TCNQ°}$_n$ as pressed pellets (±5% based upon measurements of multiple samples), indicate clearly the presence of appropriately stacked mixed-valence TCNQ's chains. The examination of the {[Ag(dmb)$_2$]TCNQ·2THF}$_n$ structure provides clues about what the structure might be. The THF density (0.899 g/cm^3 at 293 K)[28]

Table 5. Comparison of the DSC Data

	T_g/°C	ΔC_p/(J/g^{-1})	morphology
$\{[Ag(dmb)_2]TCNQ\Delta CH_2Cl_2\}_n$	25.8	0.39	crystalline
$\{[Cu(dmb)_2]TCNQ\Delta 0.25CH_2Cl_2\}_n$	25.0	0.37	semicrystalline/amorphous
$\{[Ag(dmb)_2]TCNQ{\cdot}TCNQ°\}_n$	37.7	0.19	highly crystalline
$\{[Cu(dmb)_2]TCNQ{\cdot}TCNQ°\}_n$	48.8	0.21	crystalline
$\{[Ag(dmb)_2]TCNQ{\cdot}1.5TCNQ°\}_n$	100.8	0.20	highly crystalline
$\{[Cu(dmb)_2]TCNQ{\cdot}1.5TCNQ°\}_n$	106.0	0.28	crystalline

indicates that the volume for 2THF molecules is 269.38 Å^3, which is only slightly larger than the TCNQ° volume (257.87 Å^3).[29] It seems reasonable that the replacement of 2THF molecules in the structure presented in Figure 1 by one TCNQ° could easily be achieved, with minor crystallographic modifications. This hypothesis becomes more plausible when comparing the $\{[Ag(dmb)_2]TCNQ{\cdot}1.5TCNQ\}_n$ X-ray structure described below, which is also an electric semiconducting material.

The preparation of the semiconducting $\{[M(dmb)_2]TCNQ{\cdot}1.5TCNQ°\}_n$ polymers (M = Cu, Ag) is achieved from the reactions between the 1:1 TCNQ$^-$/TCNQ° materials with an excess of TCNQ° placed as a solid at the bottom of reaction flasks. The X-ray structure for $\{[Ag(dmb)_2TCNQ{\cdot}1.5TCNQ°\}_n$ reveals a multilayer construction (Figure 4). These alternating layers consist of parallelly stacked polymers forming one layer, and a "carpet" of quasi-perpendicularly placed TCNQ's describing another (angle = 89.78°). The similarity of this structure with that of Figure 1 is obvious, where chains of TCNQ's are formed. The angle between the polymeric and TCNQ chains is 41.9°, and the TCNQ molecular axis (along the C═C bonds) is not placed parallelly to the normal plane, but exhibits an angle of ∼56°. Crystallographically, the TCNQ's form pentamers represented by colors in Figure 4 according to the sequence yellow-blue-red-blue-yellow where the red TCNQ sits on a center of symmetry, while the blues and reds are related by symmetry. The interplanar distances within this pentamer are 3.39(4) (yellow−blue) and 3.35(5) Å (blue−red), while the yellow−yellow interplanar separation is 3.29(4) Å. These distances are typical. A second TCNQ chain is depicted in this "carpet" structure. This new chain is described by the sequence blue-yellow-red-yellow-blue, and points in another direction forming an angle of ∼127° (i.e., ∼53°) with respect to the polymer chains. Some close contacts are depicted. For instance, the average distances between the yellow atoms and red TCNQ plane is 3.09(5) Å. However, poor π-contacts occur since the TCNQ's have slipped away from each other in this case. The conductivity for a pressed pellet is 2.86×10^{-2} S cm^{-1}, and compares favorably to that of the semiconducting 1:1 analogue (Table 4), suggesting similarities between the two structures.

The 1:15 TCNQ$^-$/TCNQ° stoichiometry in the semiconducting $\{[Cu(dmb)_2]TCNQ{\cdot}1.5TCNQ°\}_n$ polymers ($\sigma = 4.34 \times 10^{-4}$ S cm^{-1} for **1**, $\sigma = 6.06 \times 10^{-4}$ S cm^{-1} for **2**) is also readily demonstrated from ^{1}H NMR, UV−vis spectroscopy, and chemical analysis. The comparison of the X-ray powder diffraction patterns for M = Cu and Ag indicates extensive similarities between the two (Supporting Information), suggesting isostructurality, but the resemblance is not perfect. The Cu material is less "crystalline" than that of the Ag analogue, and the patterns provide a lesser number of scattering peaks for indexation. In this case many reasonable solutions exist, including the monoclinic system $a = 27.36$ Å, $b = 9.91$ Å, $c = 10.6$ Å, $\beta = 113.6°$, $V = 2620.9$ Å ($Z = 2$?).

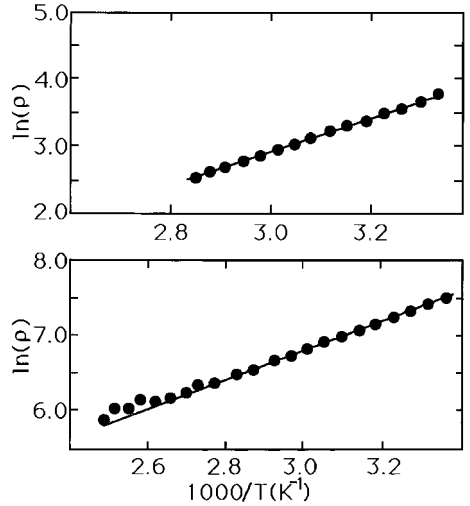

Figure 5. Graph of ln ρ (ρ = resistivity) vs 1/T for pressed pellets of $\{[M(dmb)_2TCNQ{\cdot}TCNQ\}_n$ (M = Ag, top; M = Cu (method 1), bottom).

2. Thermal Properties. The investigated materials exhibit solid-state glass transitions (Table 5), similar to that reported for the $\{[M(dmb)_2]Y\}_n$ polymers (M = Cu, Ag; Y = BF_4^-, PF_6^-, ClO_4^-, NO_3^-, $CH_3CO_2^-$).[11a] There is practically no dependence of the M and M_m on the T_g's, and the change in heat capacities (ΔC_p), but are a function of the crystallization and doping molecules. Notably, T_g increases with the size and number of these molecules, and appears to be related to TCNQ and solvation molecule motions in the solid (ordered ⇄ disordered states). The X-ray powder diffraction patterns also indicate an increase in crystallinity going from $TCNQ^-{\cdot}CH_2Cl_2$, to $TCNQ^-{\cdot}TCNQ°$, to $TCNQ^-{\cdot}1.5TCNQ°$, which in other words indicates a presence of "better organization" in the solid state. The X-ray structures reveal closer π-stacked intermolecular interactions as already shown (i.e., shorter interplanar TCNQ·· ··TCNQ distances in $TCNQ^-{\cdot}1.5TCNQ°$). The increase in T_g with the degree of "organization" is predicted easily.

3. Conductivity Properties vs Temperature. No crystal of appropriate size allowing conductivity measurements has been obtained. Instead measurements on pressed pellets were made, and indicate conductivities in the typical range for semiconducting materials. The resistivities as a function of 1/T exhibit positive slopes (Figure 5) for the $\{[M(dmb)_2]TCNQ{\cdot}TCNQ\}_n$ materials, M = Cu, Ag) confirming their semiconducting behaviors. The activation energies (E_a) extracted from the Arrhenius plots ($\rho = \rho_o \exp(E_a/kT)$) are 0.20 and 0.17 eV for M = Cu (here E_a(**1**) ≅ E_a(**2**) method 1 ∼ method 2) and Ag, respectively, and compare favorably to that known for semiconducting materials.[30−32] At ∼T_g, the resistivity increases greatly because of poor electric contacts, induced by the phase change, and at the end of each experiment the pressed pellets exhibit the electrode "fingerprints" (i.e., four pinholes).

(28) Gordon, A. J.; Ford, R. A. *The Chemist's Companion. A Handbook of Practical Data. Techniques, and References*; Wiley: New York, 1972; p. 4.
(29) Shields, L. *J. Chem. Soc., Faraday Trans. 2* **1985**, *81*, 1.
(30) Somaano, R.; Yen, S. P. S.; Rembraum, A. *Polym. Lett.* **1970**, *8*, 467.
(31) Iinuma, T.; Tanaka, T. *Inorg. Chim. Acta* **1981**, *49*, 79.
(32) Yumoto, Y.; Kato, F.; Tanaka, T. *Bull. Chem. Soc. Jpn* **1979**, *52*, 1072.

The comparison of the electric conductivity vs the molecular weight is presented in Table 4 for the {[M(dmb)$_2$]TCNQ·TCNQ°}$_n$ materials. The greater the M_n is, the lower the σ (and the crystallinity of the material) is. This observation is in fact expected for π-stacked TCNQ's, where perfectly oriented mixed-valence infinite chains are better suited for efficient electron transfer.

4. Photoconductivity. Broad band irradiation of pure pressed pellets (thickness = 3 mm) of {[Cu(dmb)$_2$]TCNQ·1.5TCNQ}$_n$ leads to a slow increase in conductivity by ~20% over a period of ~30 min, indicating the presence of photoconductivity. This process is perfectly reversible when the light source is switched on and off with the same kinetic over several days.

The mechanism for this photophysical process is deduced from the following series of experiments. First, the Ag analogue is not photoconducting. This observation suggests that the $Cu^{+/2+}$ redox couple must be involved, since the oxidation of Ag^+ into Ag^{2+} requires a more positive potential. Second, the broad band irradiation of a 1:1 mixture of {[Cu(dmb)$_2$]BF$_4$}$_n$/TCNQ° leads to a gradual color change of the pressed pellet from yellow to purple. The UV−vis spectra as a function of irradiation time for these solid-state samples exhibit a series of growing peaks at 680, 742, and 762 nm witnessing the formation of the $TCNQ^-$ anion. These two pieces of information strongly indicate the presence of a photoinduced electron transfer from the Cu^+ center to TCNQ°. To confirm this, the solid-state emission spectra and lifetimes for {[Cu(dmb)$_2$]BF$_4$}$_n$ (**2**) have been monitored as a function of added TCNQ°. In the presence of TCNQ°, the luminescence decay traces occur in a significantly shorter time frame, indicating excited-state quenching by the electron acceptor TCNQ°. Parallelly, the emission intensity (λ_{max} ~550 nm; λ_{exc} ~230 nm) also drastically decreases with the increase in TCNQ°. For instance at 25% (in weight) of TCNQ°, the emission intensity decreases by $^2/_3$, and at 10%, the intensity is at 61% of its original intensity (with no TCNQ°). The bimolecular rate constant has not been calculated since it would be meaningless in the solid state. Similar studies on the recently reported MEH−PPV polymer (poly[2-methoxy-5-(2′-ethyl-hexyloxy)-*p*-phenylenevinylene]), showed that additions of C_{60} as electron acceptor, efficiently quench the phosphorescence process of the material.[33] Practically complete disappearance of the phosphorescence band for MEH−PPV occurs with addition of 10% of C_{60}. Parallelly, no quenching of the excited-state properties for the Ag polymers by TCNQ° is observed. Thus, the quenching mechanism can be written as

$$\{Cu(dmb)_2\}_n^{n+} + h\nu \rightarrow \{Cu(dmb)_2\}_n^{n+}* \quad (1)$$

$$\{Cu(dmb)_2\}_n^{n+}* + TCNQ° \rightarrow \{Cu(dmb)_2\}_n^{(n+1)+} + TCNQ^- \quad (2)$$

On the basis of these observations, the absence of luminescence in the {[M(dmb)$_2$]TCNQ·xTCNQ°}$_n$ materials is predictable. For comparison purposes, the concentrations in TCNQ° are on the order of 10%, 20%, and 30% for x = 0.5, 1.0, and 1.5, respectively.

The facts that the Cu$_n$ backbone exhibits a long Cu···Cu separation (~5 Å) and a Cu$_3$ angle far from linearity (~140°) and that the irradiated pellets of {[Cu(dmb)$_2$]BF$_4$}$_n$ + TCNQ° (where no TCNQ chain exists) do not show a decrease in electric resistivity indicate that the mixed valent Cu$_n$ chain is not responsible for the increase in electric conductivity upon irradiation in {[Cu(dmb)$_2$]TCNQ·TCNQ°}$_n$. In fact the photoejected electron must go in the conduction band of the $TCNQ_n^{x-}$ chain.

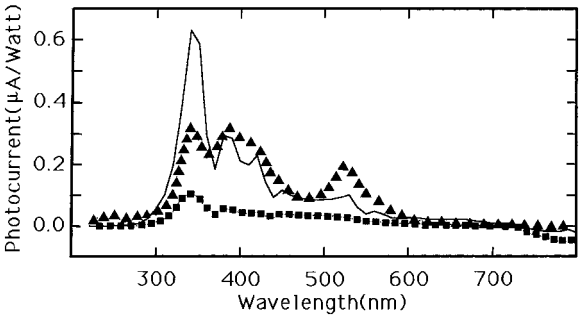

Figure 6. Spectra of the photoproduced current for the photovoltaic cells glass/SnO$_2$/{[Cu(dmb)$_2$]TCNQ·TCNQ°} + 0.5 acceptor/Al as a function of excitation wavelength (corrected for the light source and apparatus response) at full efficiency (after 20 days). Acceptor = TCNQ (▲), C_{60}(■) and TCNN (—).

The kinetic for photoinduced electron transfer is slow, as evidenced by the very long time frame necessary for the increasing photocurrent to reach an equilibrium (~30 min) with the broad band irradiation of pressed {[Cu(dmb)$_2$]TCNQ·1.5TCNQ°}$_n$ pellets. This slow kinetic is also evident from the luminescence quenching experiments ({[Cu(dmb)$_2$]BF$_4$}*$_n$ + TCNQ°) where no obvious quenching is observed in solution, even at high concentrations of TCNQ° (i.e., 1:1 Cu^+/TCNQ°). The results can be interpreted by the presence of an "insulating layer" of the dmb ligands (alkyl part) around the Cu^+ centers.

5. Photovoltaic Cells. The photovoltaic glass/SnO$_2$/polymer/Al cells are designed according to Lee et al.[34] The polymer film is made from {[Cu(dmb)$_2$]TCNQ·TCNQ°}$_n$ in the presence of 0.5 TCNQ° to form the photoconductor phase {[Cu(dmb)$_2$]-TCNQ·1.5TCNQ}$_n$.[35] The photocurrent (corrected for lamp and apparatus response) vs λ_{exc} (Figure 6), exhibits a reproducible maximum efficiency only ~20 days after the cell preparations, and this long period of time is due to a slow charge separation between the holes and electrons that occurs within the polymer film (p−n junction). This slow electron transfer kinetic is unavoidably recurrent with this material, but nonetheless, the cells are subsequently stable for at least several weeks. The low energy region below 500 nm (Figure 6) is characterized by the absence of a series of signals between 640 and 800 nm associated with the presence of $TCNQ^-$. Instead, a band located at 400 nm very likely withnesses the presence of TCNQ°. The second region (<350 nm) is the range where absorptions from the $Cu(CNR)_4^+$ centers (MLCT, metal-to-ligand charge transfer) occur.[11a] In this case, the opaque glass/SnO$_2$ substrate unavoidably cuts the excitation light off from ≤320 nm, and the apparent maximum at 330 nm is in fact and artifact. Stronger photocurrent responses are anticipated below 320 nm. The quantum yield (number of photoproduced electrons/number of photons) measured at 330 nm is 1.6×10^{-4} in this case and is significantly lower than that reported for other organometallic polymers (~1.0×10^{-2}).[36] Part of the reason for this is indeed due to the strong

(33) Sariciftci, N. S.; Braun, D.; Zhang, C.; Srdanov, V. I.; Heeger, A. J.; Stucky, G.; Sudl, F. *Appl. Phys, Lett.* **1993**, *62*, 585.

(34) Lee, S. B.; Khabibullaev, P. K.; Zakhidov, A. A.; Morita, A.; Yoshino, K. *Synth. Met.* **1995**, *71*, 2247.

(35) The true structural nature of this amorphous solid (X-ray powder diffraction) is unclear. The films still show conductivity and photoconductivity with ~50% of efficiency (2-point probes) in comparison with the pressed pellets of the crystalline materials. It is suspected that the film could be made of {[Cu(dmb)$_2$]TCNQ·xTCNQ°}$_n$ (x = 1.0 and 1.5), and TCNQ°.

absorption of the glass/SnO_2 substrate, efficiently screening the electron donor chromophores $Cu(CNR)_4^+$.

C_{60} has proven to be a good electron acceptor for other literature photovoltaic cells.[36−38] The replacement of the doping 0.5 TCNQ° by 0.5 C_{60} leads to a significant quantum yield drop (Figure 6: 5×10^{-5}; $\lambda_{exc} = 330$ nm). Being of spherical shape (diameter ∼10 Å), C_{60} does not efficiently intercalate within the TCNQ chains. The planar TCNN (13, 13, 14, 14-tetracyano-5,12-naphthacenequinodimethane; Chart 4) exhibits a reduction

Chart 4

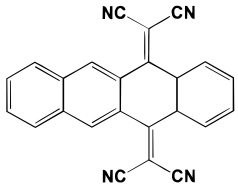

potential of −0.44 V vs SCE, slightly different from that of C_{60} (−0.60 V vs SCE).[38] The addition of 0.5 TCNN per $\{[Cu(dmb)_2]TCNQ{\cdot}TCNQ°\}_n$ in the cells, increases the quantum yield up to 3.0×10^{-4}. This result supports the hypothesis that the molecular shape of the acceptor plays in important role. Although the quantum yields are modest in comparison with other light harvesting devices.[39] The use of TCNQ or a Cu donor is made for the first time.

6. Photoreactions. The photochemical degradation of the insulating $\{[M(dmb)_2]TCNQ\}_n$ materials (M = Cu, Ag) was observed. These materials undergo very slow phototransformation (over several days) when submitted to broad band irradiation as pressed pellets (and air). The solids turn from purple to orange-brown with UV−vis spectra exhibiting a strong absorption band at ∼480 nm. For M = Ag, single crystals suitable for X-ray analysis, although of limited quality, are obtained and allowed the photoproduct identification as $\{[Ag(dmb)_2]DCTC\}_n$ (DCTC = α,α-dicyano-*p*-toluolylcyanate; Figure 7). The presence of the $DCTC^-$ can be explained from Suchanski and Van Duyne's earlier electrochemical works on $TCNQ^-$.[40] The one-electron reduction of $TCNQ^-$ occurring at −0.33V vs SCE produces the dianionic $TCNQ^{-2}$. This species turns out to be very reactive toward O_2, providing $DCTC^-$ and OCN^- via a mechanism involving a cycloaddition of O_2 onto one of the C−CN bonds.[40] Although there is no direct spectroscopic signature for $TCNQ^{-2}$ in the photochemical decompositions, IR evidence for OCN^- (ν(CN) = 2155 cm^{-1}, shoulder) and

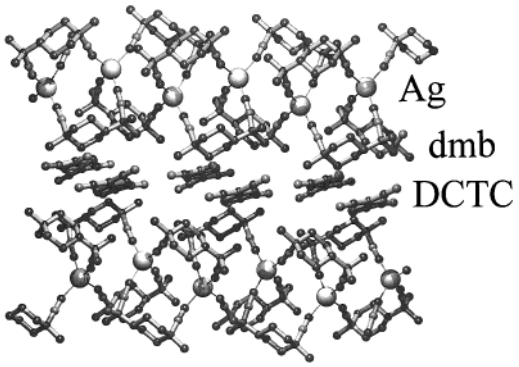

Figure 7. X-ray structure of $\{[Ag(dmb)_2]DCTC\}_n$.

$DCTC^-$ (ν(C═O) = 1645 cm^{-1}, strong) are readily observed for both polymers. No photoreaction is noticed when the pressed pellets are inserted into an airtight cell under a N_2 atmosphere.

X-ray analysis (Tables 1 and 2, Figure 7) reveals the regular $\{Ag(dmb)_2^+\}_n$ chain where all dmb ligands are in the U-shaped conformation. Both the Ag···Ag separations and Ag_3 angle are normal (i.e., ∼5 Å and ∼140°; Table 3). In this case two slightly different Ag···Ag distances are depicted. This material behaves as an electric insulator as readily predicted from the diamagnetic structure of $DCTC^-$ (and the absence of good π-stacking). The $DCTC^-$ stacks as a dimer where the O···O distance is 3.200 Å, but the two units are significantly slipped from each other (Chart 5).

Chart 5

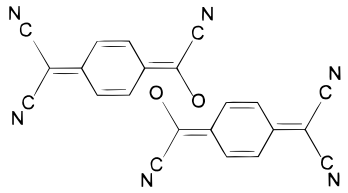

No photochemical decomposition is observed for the semiconducting $\{[M(dmb)_2]TCNQ{\cdot}xTCNQ°\}_n$ materials (M = Cu, Ag; $x = 1.0, 1.5$) under the same conditions. This observation suggests that the $TCNQ^{-2}$ does not seem to be efficiently produced either in large quantities, or for a period of time sufficiently long for subsequent reactions in these cases.

Concluding Remarks

This work reports the preparation and characterization of new $TCNQ^-$ materials involving a "rigid rod" polymeric cationic counterpart. To our knowledge this is only the second study of this sort.[12,41] Some of the materials are insulating, $\{[M(dmb)_2]TCNQ{\cdot}xTCNQ°{\cdot}solvent\}_n$ (M = Cu, Ag; $x = 0, 0.5$), and others are semiconducting, $\{[M(dmb)_2]TCNQ{\cdot}xTCNQ°\}_n$ (M = Cu, Ag; $x = 1.0, 1.5$), depending upon whether mixed valence TCNQ chains are formed or not. In all cases, T_g's are observed. These unprecedented results for relatively crystalline polymers are dependent upon the amount of "*x*TCNQ°·solvent" materials. In one case, $\{[Cu(dmb)_2]TCNQ{\cdot}1.5TCNQ°\}_n$, a photoconducting material is obtained, and photophysical and spectroscopic

(36) Köhler, A.; Wittmann, H. F.; Friend, R. H.; Khan, M. S.; Lewis, J. *Synth. Met.* **1994**, *67*, 245.
(37) Janssen, R. A. J.; Christiaans, M. P. T.; Hare, C.; Martin, N.; Saricifti, N. S.; Heeger, A. J.; Wudl, F. *J. Chem. Phys.* **1995**, *103*, 8840.
(38) The first reduction potentials for TCNQ, C_{60} and TCNN are as follow: 0.08 V vs SCE in 0.2 M $Bu_4N(ClO_4)/CH_3CN$, −0.60 V vs SCE in 0.1 M $Bu_4N(ClO_4)$/toluene/CH_3CN (5: 1), and −0.44 V vs SCE in 0.2 M $Bu_4N(ClO_4)/CH_3CN$, respectively. See: Martin, N.; Behnish, R.; Hanack, M. *J. Org. Chem.* **1989**, *54*, 2563. Illescas, B.; Martin, N.; Seoane, C. *Tetrahedron Lett.* **1997**, *38*, 2015.
(39) See, for instance: (a) O'Reagan, B.; Grätzel, M. *Nature* **1991**, *353*, 737. (b) Bard, A. J. *J. Photochem.* **1979**, *10*, 59. (c) Wrighton, M. S. *Acc. Chem. Res.* **1979**, *12*, 303. (d) Heller, A. *Acc. Chem. Res.* **1981**, *14*, 154. (e) Abruna, H. D.; Bard, A. J. *J. Am. Chem. Soc.* **1981**, *103*, 6898. (f) Archer, M. D.; Bolton, J. R. *J. Phys. Chem.* **1990**, *94*, 8028. (b) Borja, M.; Dutta, P. K. *Nature* **1993**, *362*, 43. (h) Khaselev, O.; Turner, J. A. *Science* **1998**, *280*, 425. (i) Oregan, B.; Grätzel, M. *Nature* **1991**, *353*, 737. (j) Moser, J. E.; Bonnote, P.; Grätzel, M. *Coord. Chem. Rev.* **1998**, *171*, 245. (k) Grätzel, M. *Coord. Chem. Rev.* **1991**, *111*, 167. (l) Argazzi, R.; Bignozzi, C. A.; Hasselmann, G. M.; Meyer, G. J. *Inorg. Chem.* **1998**, *37*, 4533.
(40) Suchanski, M. R.; Van Duyne, R. P. *J. Am. Chem. Soc.* **1976**, *98*, 250.
(41) We recently reported the preparation of the polynuclear complex $[Ag_4(dmb)_4(TCNQ)_3]TCNQ$ which consists of an infinite $(TCNQ^-)_n$ chain where a series of "$Ag_2(dmb)_2^{2+}$" fragments are stacked side by side interacting with the $TCNQ^-$ via Ag^+···NC− weak bondings. The Ag^+ ions are not saturated in this case, and allows $TCNQ^-$···Ag^+ interactions. See Fortin, D.; Drouin, M.; Harvey, P. D.; Herring, F. G.; Summers, D. A.; Thompson, R. C. *Inorg. Chem.* **1999**, *38*, 1253.

studies indicate that photoinduced conductivity is promoted via an electron transfer from the excited Cu(CNR)$_4^+$ center to TCNQ acceptors. To take advantage of the photoconductivity property, a series of photovoltaic cells are designed. The efficiency is optimal in the UV region, which is consistent with the nature of the Cu(I) chromophore, but the overall performance of the cell is modest, and kinetic is slow.

One solution to this problem is, of course, the use of the performing semi-transparent and semiconducting indium-containing tin oxide material (ITO) on a quartz substrate. However more important problems should be addressed concerning both the thermodynamic and kinetic aspects of the cell. The driving force for electron transfer should be improved. Recently our group prepared polymers of the type {[M$_4$(dmb)$_4^{2+}$](L−L)}$_n$ (M = Pd, Pt; L−L = dmb, PPh$_2$(CH$_2$)$_m$PPh$_2$, m = 4, 5, 6) where 84 000 < M_n < 30 700.[42] Preliminary results show that the M$_4$(dmb)$_4^{2+}$ donor is a better donor than Cu(CNR)$_4^+$, potentially providing a greater driving force for electron transfer. On the basis of the morphology results, the more crystalline Ag−polymers are better conductors than the Cu analogues. Likewise, local TCNQ chain order is important for electron delocalization. The preparation of mixed {Cu$_x$Ag$_y$(dmb)$_2^+$}$_n$ polymers ($x + y = 1.0$) should provide materials of high crystallinity levels related to {Ag(dmb)$_2^+$}$_n$ properties, but at the same time, they should exhibit the photoconductivity properties associated with the presence of Cu(I) centers. In addition, bridging ligands of the type *p*-diethynylbenzene and *p*-diisocyanobenzene should provide orbital connectivity necessary for intrapolymer chain conductivity.

Acknowledgment. This research was supported by the Natural Sciences and Engineering Research Council of Canada and the Fonds Concertés pour l'Avancement de la Recherche.

Supporting Information Available: Tables listing detailed crystallographic data, atomic positional parameters, bond lengths and angles, anisotropic displacement parameters, hydrogen coordinates and isotropic displacement parameters, torsion angles, tables of least-squares planes and deviations, ORTEP figures, figures showing X-ray powder diffraction patterns, and tables of indexation data. This material is available free of charge via the Internet at http://pubs.acs.org.

IC990975O

(42) (a) Zhang, T.; Drouin, M.; Harvey, P. D. *Inorg. Chem.* **1999**, *38*, 1305. (b) Zhang, T.; Drouin, M.; Harvey, P. D. *Inorg. Chem.* **1999**, *38*, 957.